VIP Shape-Memory Porous Films Very Important Paper

International Edition: DOI: 10.1002/anie.201712100
German Edition: DOI: 10.1002/ange.201712100

Light-Driven Shape-Memory Porous Films with Precisely Controlled Dimensions

Wei Wang, Dingfeng Shen, Xiao Li, Yuan Yao, Jiaping Lin, Aurelia Wang, Jiwoo Yu, Zhong Lin Wang, Suck Won Hong, Zhiqun Lin, and Shaoliang Lin**

Abstract: *Shape-memory polymers (SMPs) are an intriguing class of smart materials possessing reversible shape change and recovery capabilities. Effective routes to shape-memory porous films (SMPFs) are few and limited in scope owing to the difficulty in manipulating the shape change of pores by conventional methods. Herein we report an unconventional strategy for crafting light-driven SMPFs by judiciously constructing highly ordered porous films via a facile "breath figure" approach, followed by sequential vapor crosslinking and nondestructive directional light manipulation. Micropores can thus be transformed into other shapes including rectangle, rhombus and size-reduced micropores at room temperature. The transformed micropores can be reverted to their original shapes by either thermal annealing or UV irradiation. As such, this strategy expands the rich diversity of SMPs accessible.*

Shape-memory polymers (SMPs) are widely recognized as smart materials which can memorize their original shape, and revert to their pre-deformed shape by external stimulus, such as temperature, light, pH, electric field, and magnetic field.[1] A prerequisite for SMPs is to construct a two-phase system, that is, a stable network-like phase for immobilizing the original shape and stabilizing the entire SMPs and a reversible phase that can be easily deformed and recovered by external stress and stimulus.[2] It is important to note that despite multifarious effective routes to reverse the deformed phase, the initial deformation process from the original shape to temporary shape is primarily accomplished mechanically.[3] Thus, it is difficult to conduct and produce uniform deformation over bulk polymeric materials. Furthermore, once the original shape is recovered, a new mechanical processing step is required to rebuild the temporary shape.[4] Instead of by exerting external forces, the smarter SMPs would have the capability to reform their temporary shapes by internal driving forces triggered by stimuli.[5]

Porous polymer films with uniform pores have garnered significant attention as they offer a wide spectrum of applications as membranes for separation and purification, low-dielectric constant materials for microelectronic and photonic devices, and solid catalyst and sensor supports.[6] The pore size, shape, and uniformity as well as the film reusability exert profound influence on the properties and applications of porous films.[7] Crafting shape-memory porous films (SMPFs) would certainly carry a number of advantages (e.g., controllable shape and size, reutilization) for their applications. However, due largely to the challenge of homogeneously deforming (i.e., reshaping) pores, the ability to create SMPFs with ordered pores remains very limited.[8] More notably, light-driven SMPFs have not yet been explored.

Azobenzene-containing compounds are an intriguing class of molecules that undergo reversible *trans*-to-*cis* isomerization upon UV (i.e., *trans*-to-*cis*) or visible light (i.e., *cis*-to-*trans*) irradiation.[9] Azobenzene-containing polymers can experience polarized light-induced photo-alignment and UV light-induced anisotropic-to-isotropic transition.[10] Recently, we developed a directional light manipulation (DLM) technique to tailor the surface features of azobenzene-containing porous polymer films with uniform micropores formed by the so-called "breath figure" method (where a breath figure is the water droplet array that forms when moisture comes in contact with a cold substrate).[11] Under polarized light irradiation, the azobenzene units undergo photo-alignment, thus inducing the directional mass migration of polymer. By tuning the polarization direction of linearly polarized light (LPL), the original round micropores can be readily converted into a rich variety of shapes, including rectangle, rhombus and parallelogram. More interestingly, circularly polarized light was found to impart the manipulation of size and wall thickness of micropore while retaining its shape.[12] Thus, DLM may serve as a robust platform for noncontact and nondestructive reshaping of microstructures.[13] Herein, light-driven SMPFs with exquisitely controlled dimensions were crafted, for the first time, via a three-step strategy, namely, construction of porous film by the "breath figure" approach, creation of stable network phase by crosslinking polymer chains, and DLM of the reversible phase by linearly or circularly polarized light at room temperature. For the preparation of SMPFs, the micro-

[*] W. Wang, D. Shen, Dr. Y. Yao, Prof. J. Lin, Prof. S. Lin
Shanghai Key Laboratory of Advanced Polymeric Materials, Key Laboratory for Ultrafine Materials of Ministry of Education, School of Materials Science and Engineering, East China University of Science and Technology
Shanghai, 200237 (China)
E-mail: slin@ecust.edu.cn
W. Wang, X. Li, A. Wang, J. Yu, Prof. Z. L. Wang, Prof. Z. Lin
School of Materials Science and Engineering
Georgia Institute of Technology
Atlanta, GA 30332 (USA)
E-mail: zhiqun.lin@mse.gatech.edu
Prof. S. W. Hong
Department of Cogno-Mechatronics Engineering, Department of Optics and Mechatronics Engineering, Pusan National University
Busan, 46241 (Republic of Korea)
Supporting information and the ORCID identification number(s) for the author(s) of this article can be found under: https://doi.org/10.1002/anie.201712100.

pores reshaped by DLM undergo shape recovery upon either UV irradiation or thermal annealing above T_g. This light-driven shape-memory process can proceed repeatedly, dispensing the need for any external forces. This study represents the first demonstration of capitalizing on the "breath figure" route to prepare light-driven SMPFs with controllable size and shape.

Diblock copolymer poly(4-vinylpyridine)-*block*-poly-[6-[4-(4-butyloxyphenylazo)phenoxy]hexyl methacrylate] (denoted P4VP-*b*-PAzoMA) with the molecular weight of 2.67×10^4 g mol^{-1} and the weight fraction of PAzoMA of 54.4% was synthesized by a two-step reversible addition–fragmentation chain transfer polymerization (see Supporting Information and Table S1).[11] The chemical structure of P4VP-*b*-PAzoMA diblock copolymer consisting of a crosslinkable P4VP block and a photo-responsive PAzoMA block is shown in the inset of Figure S1 in the Supporting Information. A honeycomb film composed of P4VP-*b*-PAzoMA diblock copolymer was then produced via the a "breath figure" process (see Supporting Information).[14] A representative optical micrograph of porous film possessing hexagonally packed micropores (i.e., honeycomb film) over a large area is shown in Figure S1. The honeycomb film exhibited a nacre color due to the sunlight diffraction and interference (lower-left inset in Figure 1b). The scanning electron microscopy (SEM) images (in Figure 1b) and atomic force microscopy (AFM) image (Figure 1c) revealed a highly regular hexagonal array of uniform monolayer-thick spherical micropores with a diameter (d) of 2.50 ± 0.05 μm and a center-to-center distance (D) between two adjacent micropores of 2.95 ± 0.06 μm.

As noted above, a stable network phase is required to immobilize the original shape and stabilize the entire polymer system during the shape memory process. In this context, 1,4-diiodobutane (DIB) vapor was used as crosslinker and reacted with pyridyl groups from two adjacent P4VP chains in honeycomb film via a vapor–solid intermolecular quaterisation reaction (Figure 1a), yielding the crosslinked honeycomb film (Figure 1d). To quantify the degree of quaterisation, X-ray photoelectron spectroscopy (XPS) was carried out on the honeycomb film (Figure S2a). The relative degree of quaterisation of pyridyl groups was determined as the ratio of quaternized area to the overall areas of N1s electrons (see inset of Figure 1e and Figure S2b).[15] Upon exposure to DIB, quaterisation degree was first increased with time and then remained nearly unchanged at 23.5% after 6 h (Figure 1e). Moreover, Fourier transform infrared spectroscopy in Figure S3a also indicated quaterisation.[16]

Note that compared with as-prepared sample (Figure 1b), no obvious morphological change was observed on the crosslinked honeycomb film (Figure 1d). According to the DSC measurements (Figure S3b), a slight increase of glass transition temperature T_g from 79.0 °C to 81 °C was seen after crosslinked for 6 h, due likely to the relatively low crosslinking density. However, the crosslinked films possessed significantly improved stability upon heating and solvent treatments (Figure S4 and Figure S5). The markedly improved stability of crosslinked films render them shape memory capability and practical utilization.

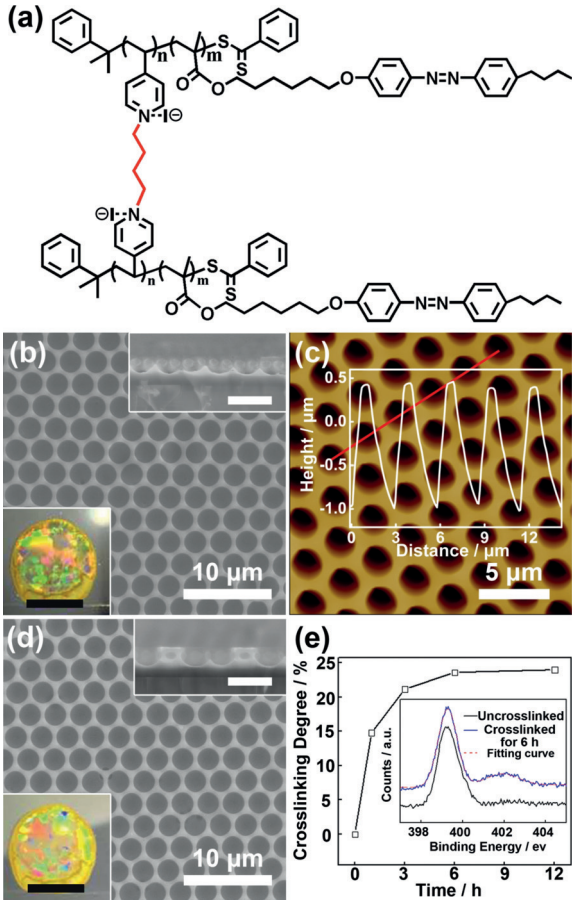

Figure 1. Formation and crosslinking of honeycomb film composed of P4VP-*b*-PAzoMA diblock copolymers. a) Chemical structures of crosslinked P4VP-*b*-PAzoMA diblock copolymers, crosslinker is marked in red. b) SEM images of as-prepared honeycomb film (inset lower-left: photograph of the sunlight diffraction of the film, black scale bar = 5 mm; inset upper-right: SEM cross-sectional view of the film, white scale bar = 5 μm). c) AFM height image of as-prepared honeycomb film (inset: the height profile of the line scan in red). d) SEM images of the DIB-crosslinked honeycomb film (inset lower-left: photograph of the sunlight diffraction of the film, black scale bar = 5 mm; inset upper-right: SEM cross-sectional view of the film, white scale bar = 5 μm). e) Quaterisation degree of the film determined by XPS (inset: nitrogen 1s region of the films, the red dotted line is the corresponding Gaussian fit to the XPS spectrum for the sample crosslinked by DIB for 6 h.

For the photo-switchable properties as discussed above, azobenzene-containing polymers are promising candidates for reversible phase in SMPs. To this end, our recently developed DLM technique was implemented to tailor the surface feature of honeycomb films. Figure 2a depicts a vertical incident linearly polarized visible light (hereafter referred to as LPL) irradiated on the honeycomb film. Owing to the directionality of light-induced mass migration, two characteristic polarization directions of LPL irradiation defined as the V direction (parallel to the hexagonal wall of the micropore array; Figure 2a) and S direction (perpendicular to hexagonal wall), respectively, were chosen to conduct the DLM. For as-prepared (i.e., uncrosslinked) film, remarkable micropore deformation (i.e., reshaping) was occurred

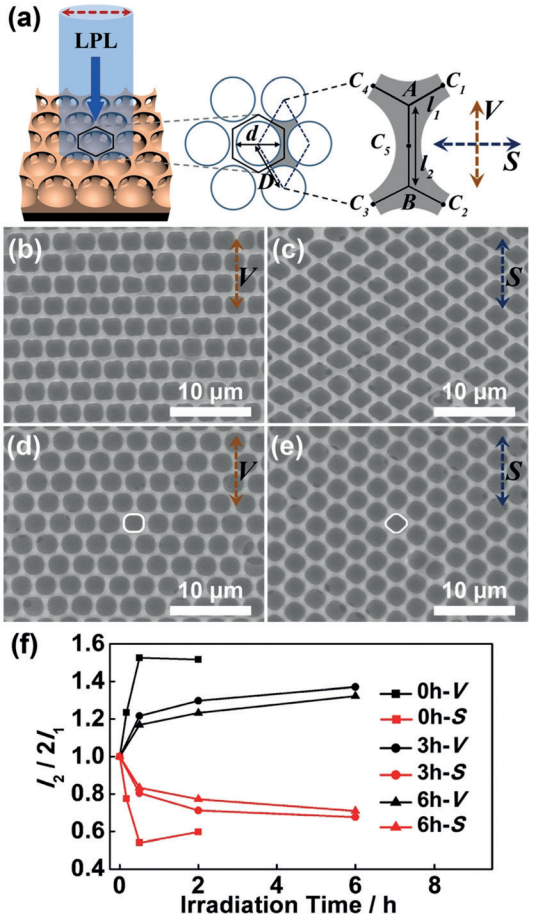

Figure 2. LPL-induced reshaping of micropores in honeycomb films. a) Schematic illustration of the definition of a unit cell and two types of LPL irradiation, see text for details. SEM images of as-prepared honeycomb films upon LPL irradiation for 30 mins: b) along the V direction and c) along the S direction. SEM images of crosslinked honeycomb films (i.e., after crosslinked by DIB vapor for 6 h) upon LPL irradiation for 6 h: d) along the V direction and e) along the S direction. An individual round–rectangular micropore and round–rhombic micropore are marked in white for guidance in (d) and (e), respectively. f) Plots of $l_2/2l_1$ of honeycomb films obtained at different crosslinking times versus the LPL irradiation times in two modes of irradiation.

upon irradiation for 30 min (Figure 2b,c). Round micropores were reshaped into rectangular micropores upon V-polarized LPL irradiation (Figure 2b), while the S-polarized LPL converted the micropores into rhombic shape (Figure 2c). In contrast, for DIB-crosslinked honeycomb films, DLM also conferred the reshaping but with a smaller degree than that in the uncrosslinked film, which can be ascribed to the crosslinking of P4VP chains, thus yielding round–rectangular micropores upon V-polarized LPL irradiation (Figure 2d) and round–rhombic micropores upon S-polarized LPL irradiation (Figure 2e).

We now turn our attention to quantify the extent of deformation in as-prepared and crosslinked honeycomb films. In a unit cell (rhombic area, dashed box in central panel; Figure 2a) of honeycomb film, barycenters of the triangle-connected micropores are denoted points A and B, and middle points of adjacent micropores are denoted point C (right panel in Figure 2a). The value of l_2 (length between points A and B) and l_1 (length between a barycenter and its adjacent middle point C) were varied upon DLM as a result of micropore reshaping. Therefore, $l_2/2l_1$ was calculated to measure the reshaping degree of micropores as a function of LPL irradiation time as summarized in Figure 2f. The consequence of light-induced mass migration is manifested in the expansion and elongation of polymers along the light polarization direction and accompanied by the contraction against the polarization direction owing to the isovolumetric effect.[11,17] Under V-polarized LPL irradiation, the polymer wall of unit cell tended to be stretched along the AB direction (right panel in Figure 2a). Thus, the barycenters A and B were pulled away from each other, leading to increased l_2 and decreased l_1 (i.e., $l_2/2l_1 > 1$) and creating rectangular micropores. Conversely, for S-polarized LPL irradiation, the polymer wall preferred to contract along the AB direction. The barycenters A and B approached one another, resulting in rhombic micropores with decreased l_2 and increased l_1 (i.e., $l_2/2l_1 < 1$). Notably, for as-prepared honeycomb film, the reshaping degree increased rapidly at the early stage (e.g., 0.5 h; squares in Figure 2f) and then decreased after lengthy LPL irradiation owing to the collapse of surface structure generated by photofluidization effect (e.g., 6 h; Figure S6).[18] For the crosslinked films, the reshaping degree increased progressively as a function of irradiation time (circles and triangles in Figure 2f, Figure S7). It is also notable that longer-time crosslinking resulted in slower deformation (reshaping) speed. Moreover, the crosslinked network also suppressed photofluidization effect, thus preventing the occurrence of irreversible collapse (inset in Figure S7d, where no structural collapse was seen). Clearly, DLM technique affords a powerful platform to reshape the crosslinked films without the collapse of micropores. It is notable that LPL with specific wavelength (i.e., blue-green LPL) should be employed in the DLM process to activate simultaneous *trans*-to-*cis* and *cis*-to-*trans* isomerizations for photoalignment and the following directional mass migration of azopolymer.[19] The light intensity has a great influence on reshaping speed of pores. Typically, a slower reshaping speed will be encountered under a weaker LPL irradiation.[11]

For crafting SMPFs, two-phase system and DLM-induced pore reshaping have been achieved above. Subsequently, the resulting honeycomb films with round–rectangular and round–rhombus micropores (Figure 2d,e) were subjected to thermal annealing and UV irradiation to recover their original shape (i.e., round) as depicted in Figure 3a (see Supporting Information). The reshaped micropores (Figure 2d) were first thermally annealed above T_g ($T_g = 81\,^{\circ}C$), in situ optical microscopy observation of round-rectangular micropores is shown in Figure 3b–d and Figure S8. A gradual shape recovery from round–rectangular to round was observed after thermal annealing for 2 h, which agreed well with the slow shape-recovery behavior induced by glass transition. The inset in Figure 3e shows that the ratio of $l_2/2l_1$ underwent a rapid decrease from 1.29 to 1.05 in the first 5-min thermal annealing and then slowly approach 1 as the thermal annealing time progressed. The SEM and AFM height images

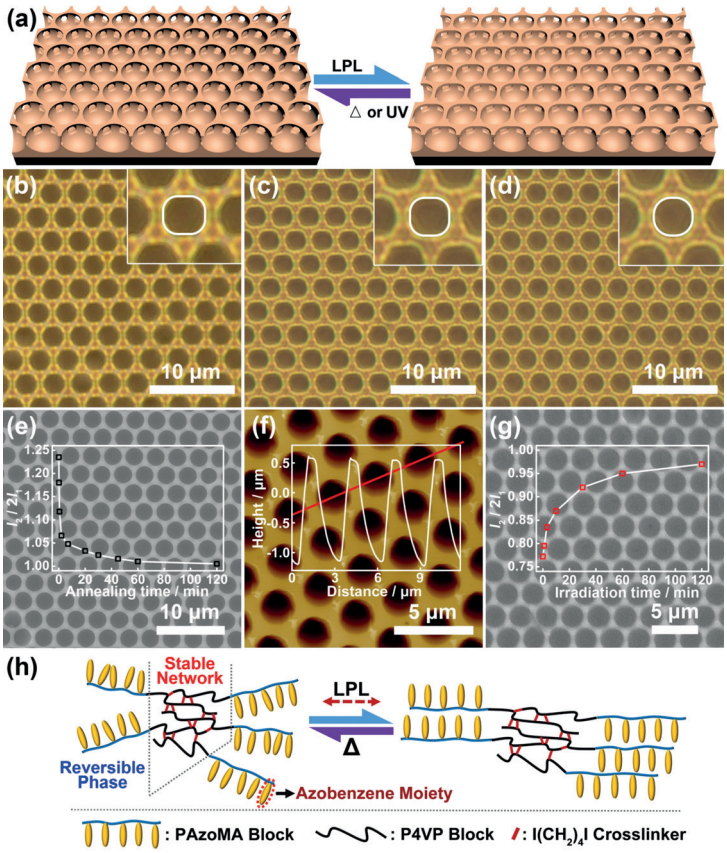

Figure 3. Shape recovery of reshaped honeycomb films by either thermal annealing or UV irradiation. a) The schematic representation of the reversible morphological change between deformed (right) shape upon LPL irradiation and original (left) shape upon thermal annealing or UV irradiation. b)–d) Thermal annealing-induced recovery of the reshaped honeycomb film monitored by optical microscopy: b) reshaped round-rectangular micropores; c) after thermal annealing for 30 s; and d) after thermal annealing for 20 min. Insets in (b–d) are the magnified micropores with an individual micropore marked in white for guidance. e),f) Morphology of a fully recovered film after thermal annealing: e) SEM image of 2-h thermally annealed film (inset: the ratio of $I_2/2I_1$ vs. the annealing time); and f) AFM height image of 2-h thermally annealed film (inset: the cross-sectional profile of micropores scanned along the red line). g) SEM image of 2-h UV-irradiated honeycomb film (inset: the calculated $I_2/2I_1$ vs. the UV irradiation time). h) Schematic illustration of change of polymer chain conformations in a two-phase system of SMPFs: LPL-induced deformation process and thermal annealing-induced recovery process. Note: all honeycomb films were crosslinked prior to the reshape and recovery processes.

(Figure 3e,f, respectively) for the 2-h thermally-annealed film displayed a complete recovery of its original round shape without any change of micropore size. More importantly, the shape recovery of rhombic micropores (Figure 2e) by UV irradiation was also demonstrated by in situ optical microscopy observation and summarized in Figure S9. A smooth recovery of $I_2/2I_1$ from 0.77 to 0.97 upon UV irradiation for 2 h was shown as the inset in Figure 3g. The increased $I_2/2I_1$ and SEM image in Figure 3g suggested the restoration of round shape after UV irradiation.

On the basis of reshaping and recovery processes discussed above, robust light-driven SMPFs were thus crafted. Based on the calculation of order parameter S of *trans*-state azobenzene moieties from polarized absorbance of spin-coated film (Figure S10, Figure S11, and Equation S1), we proposed a model to elucidate the change of polymer chain conformations during the shape-memory process, as depicted in Figure 3h. Clearly, the crosslinked P4VP blocks in honeycomb film were served as stable network phase, which immobilized the original round shape of micropores. Moreover, during the shape deformation and recovery process, this stable network phase stabilized the crafted SMPFs and prevented them from collapse. On the other hand, flexible PAzoMA blocks (uncrosslinked) functioned as the reversible phase for rendering photoresponsive properties. Prior to deformation by LPL irradiation, PAzoMA chains are randomly distributed in honeycomb film (i.e., isotropic state, $S = 0$) as depicted in the left side of Figure 3h (verified in Figure S12 and Figure S13a). During the 2-h DLM process, S gradually increases from 0 to 8.68% (Figure S13a and Figure S13d), indicating that PAzoMA chains are oriented by LPL due to the photo-induced alignment of azobenzene moieties on PAzoMA chains (right side of Figure 3h), which impart the directional mass migration and the micropore reshaping. Subsequently, S decreased to 0 upon subsequent thermal annealing or UV irradiation (Figure S13b–d), suggesting these aligned PAzoMA chains revert to their original isotropic state, thus enabling the shape recovery.

In addition to LPL-manipulated pores, size-reduced micropores generated by circularly polarized light (CPL) irradiation can also be recovered by thermal annealing or UV light irradiation (Figure S14), demonstrating the ability to reversibly manipulate the pore size by designing SMPFs. More importantly, due to the light-driven and nondestructive property, the above shape memory process can be repeated many times without any external force (Figure S15 and Figure S16). Furthermore, the origin shape of micropores can be fixed at any stage during the reshaping of round micropores of uncrosslinked honeycomb films (Figure S17). Clearly, this facile vapor–solid crosslinking strategy may offer great flexibility and feasibility in creating the SMPFs with a rich variety of original shapes.

In summary, we developed a viable strategy by judiciously integrating a "breath figure" process, selective vapor-crosslinking, and directional light manipulation at room temperature to form the first light-driven SMPFs. Clearly, the created light-driven SMPFs displayed tunable and recoverable pore size and shape with good reusability. A model based on the change of polymer chain conformations during the shape-memory process was proposed by measuring the anisotropy in the two-phase system, providing insight into photo-induced mass migration and shape recovery process. In sharp contrast to traditional SMPs which commonly rely on mechanically induced shape change and thermally triggered shape recovery, this study presents a new means of designing and capitalizing on SMPs that can be remotely and non-destructively light-manipulated for reshaping with a finer

level of structural control and then either thermal or light activated materials for shape recovery. This strategy for light-driven SMPs opens up exciting opportunities for creating a large variety of light-driven shape-memory microstructures possessing different dimensions, compositions and functionalities. Such light-driven SMPFs may find potential applications as smart membranes for efficient separation and purification, masks for pattern transfer, scaffolds for tissue engineering, and controlled release of drugs, cosmetics, inks, or chemical reagents.

Acknowledgements

This work is supported by National Natural Science Foundation of China (grant nos. 51622301 and 51573046) and the National Science Foundation (CMMI 1727313). Support from Projects of Shanghai Municipality (14SG29, 222201717001 and 17JC400700) and National Research Foundation of Korea (BK21 Plus program) are also appreciated.

Conflict of interest

The authors declare no conflict of interest.

Keywords: azobenzene · block copolymers · light manipulation · shape memory · thin films

How to cite: *Angew. Chem. Int. Ed.* **2018**, *57*, 2139 – 2143
Angew. Chem. **2018**, *130*, 2161 – 2165

[1] a) A. Lendlein, S. Kelch, *Angew. Chem. Int. Ed.* **2002**, *41*, 2034 – 2057; *Angew. Chem.* **2002**, *114*, 2138 – 2162; b) Q. Zhao, H. J. Qi, T. Xie, *Prog. Polym. Sci.* **2015**, *49 – 50*, 79 – 120.
[2] N. Zheng, Z. Fang, W. Zou, Q. Zhao, T. Xie, *Angew. Chem. Int. Ed.* **2016**, *55*, 11421 – 11425; *Angew. Chem.* **2016**, *128*, 11593 – 11597.
[3] Y. Liu, J. Genzer, M. D. Dickey, *Prog. Polym. Sci.* **2016**, *52*, 79 – 106.
[4] a) T. Lv, Z. Cheng, E. Zhang, H. Kang, Y. Liu, L. Jiang, *Small* **2017**, *13*, 1503402; b) L. Zhao, J. Zhao, Y. Liu, Y. Guo, L. Zhang, Z. Chen, H. Zhang, Z. Zhang, *Small* **2016**, *12*, 3327 – 3333.
[5] a) S.-Q. Wang, D. Kaneko, M. Okajima, K. Yasaki, S. Tateyama, T. Kaneko, *Angew. Chem. Int. Ed.* **2013**, *52*, 11143 – 11148; *Angew. Chem.* **2013**, *125*, 11349 – 11354; b) Y. Hu, W. Guo, J. S. Kahn, M. A. Aleman-Garcia, I. Willner, *Angew. Chem. Int. Ed.* **2016**, *55*, 4210 – 4214; *Angew. Chem.* **2016**, *128*, 4282 – 4286.
[6] J. Li, Y. Zhang, *Chem. Mater.* **2007**, *19*, 2581 – 2584.
[7] K. R. Phillips, N. Vogel, Y. Hu, M. Kolle, C. C. Perry, J. Aizenberg, *Chem. Mater.* **2014**, *26*, 1622 – 1628.
[8] a) Y. Fang, Y. Ni, S.-Y. Leo, C. Taylor, V. Basile, P. Jiang, *Nat. Commun.* **2015**, *6*, 7416; b) Y. Fang, Y. Ni, B. Choi, S.-Y. Leo, J. Gao, B. Ge, C. Taylor, V. Basile, P. Jiang, *Adv. Mater.* **2015**, *27*, 3696 – 3704.
[9] E. M. M. Tan, S. Amirjalayer, S. Smolarek, A. Vdovin, F. Zerbetto, W. J. Buma, *Nat. Commun.* **2015**, *6*, 5860.
[10] H. Yu, T. Kobayashi, *Molecules* **2010**, *15*, 570.
[11] W. Wang, C. Du, X. Wang, X. He, J. Lin, L. Li, S. Lin, *Angew. Chem. Int. Ed.* **2014**, *53*, 12116 – 12119; *Angew. Chem.* **2014**, *126*, 12312 – 12315.
[12] W. Wang, Y. Yao, T. Luo, L. Chen, J. Lin, L. Li, S. Lin, *ACS Appl. Mater. Interfaces* **2017**, *9*, 4223 – 4230.
[13] a) F. Pirani, A. Angelini, F. Frascella, R. Rizzo, S. Ricciardi, E. Descrovi, *Sci. Rep.* **2016**, *6*, 31702.
[14] H. Bai, C. Du, A. Zhang, L. Li, *Angew. Chem. Int. Ed.* **2013**, *52*, 12240 – 12255; *Angew. Chem.* **2013**, *125*, 12462 – 12478.
[15] R. C. Hayward, B. F. Chmelka, E. J. Kramer, *Macromolecules* **2005**, *38*, 7768 – 7783.
[16] B. P. Tripathi, N. C. Dubey, S. Choudhury, F. Simon, M. Stamm, *J. Mater. Chem. B* **2013**, *1*, 3397 – 3409.
[17] P. Karageorgiev, D. Neher, B. Schulz, B. Stiller, U. Pietsch, M. Giersig, L. Brehmer, *Nat. Mater.* **2005**, *4*, 699 – 703.
[18] S. Lee, H. S. Kang, A. Ambrosio, J.-K. Park, L. Marrucci, *ACS Appl. Mater. Interfaces* **2015**, *7*, 8209 – 8217.
[19] J. Bin, W. S. Oates, *Sci. Rep.* **2015**, *5*, 14654.

Manuscript received: November 24, 2017
Accepted manuscript online: January 11, 2018
Version of record online: January 29, 2018

